An Improved Forward Scattering Simulation Technique for Microwave Breast Imaging

B. Babu and M. Condon

RINCE, School of Electronic Engineering, Dublin City University, Dublin 9, Ireland

Abstract— Microwave imaging is a promising alternative to conventional mammography methods. At microwave frequencies, normal and malignant tissues show high contrasts in their electrical properties. Microwave Imaging (MWI) systems can be used to construct three-dimensional profiles of the electrical properties of the body part that is being examined. MWI systems illuminate the body part with electromagnetic radiation of a suitable frequency. Using the measured scattered field at the surface of the body, inverse scattering algorithms reconstruct profiles of the electrical properties of the target. It is therefore of the uttermost importance that the forward scattering set-up is correct so that an inversion algorithm can create accurate profiles of electrical properties. We propose an improvement over the existing integral equation based forward scattering simulation techniques for microwave breast cancer imaging. Early detection of breast cancer is crucial. At this stage, the size of malignant tissue can be in the order of millimeters. For imaging involving such a small malignancy, one must use high-frequency radiation. At such frequencies, in order to overcome the relaxation effect of complex permittivity, we use the Debye model. For solving the forward scattering problem, we use the stabilized bi-conjugate gradient fast Fourier transform method (BI-CGSTAB-FFT). For the scattering domain, we apply the so-called cyclic boundary condition. This reduces the number of FFTs involved thus saving time and memory. For the BI-CGSTAB-FFT iteration method, we choose the initial value of the total field to be the incident electric field. This choice yields better convergence than a random selection of initial condition.

1. INTRODUCTION

Current imaging techniques for the early detection of breast cancer include X-rays, MRI and ultrasound imaging. X-ray mammography is the most common method employed at present. However, it poses certain health risks owing to the ionizing nature of the radiation. In addition, the method has relatively high false detection rates [1, 2]. Recently, microwave imaging has been proposed as a painless alternative to conventional X-ray mammography. Its non-ionizing nature makes it a safe probing method for the patient. In addition, the relatively lower manufacturing and maintenance cost makes it a viable economic replacement for conventional mammography machines. Studies have shown that at microwave frequencies, normal and malignant tissues show reasonable contrast in their electrical properties [3]. A recent large-scale study [4] reveals more insight into the electrical properties of the breast tissues. According to [4], there is no significant difference among the dielectric properties of breast tissue samples obtained from a large number of patients. This finding strengthens the case for using the MWI for identifying malignant regions as for all patients, regions with high contrast in dielectric properties will indicate abnormalities in normal tissues. Accurate simulation of the underlying scattering problem is of immense importance. These simulations facilitate the design and development of suitable imaging chambers, the selection of better antennas and efficient image reconstruction algorithms.

Simulation of electromagnetic problems at microwave frequencies is challenging as the size of governing matrix equations grows with frequency. Any improvement in algorithms that reduces the computation time or memory usage is of immense benefit. In this paper, we include cyclic boundary conditions [7] in the discretization procedure which reduces overall computation time and memory requirements while the accuracy is not affected. At high frequencies, in order to overcome the relaxation effect of complex pemittvity, we use the single-pole Debye dispersion expression [9].

2. SIMULATION SETUP

MWI involves the scattering of microwave radiation by an inhomogeneous body and the reconstruction of three-dimensional (3-D) maps of the dielectric properties of the target using the measured scattered field. In this study, we use an inhomogeneous sphere of radius 0.064 m as shown in Fig. 1

as the scatterer to mimic the breast. The forward scattering problem is modelled with the volume electric field integral equation approach of scattering theory. The source of microwave radiation is an electric dipole placed at $z = -0.08\,\mathrm{m}$ as shown in Fig. 1. In the spherical polar coordinate system, the expression for the electric field due to an electric dipole is given by [5]:

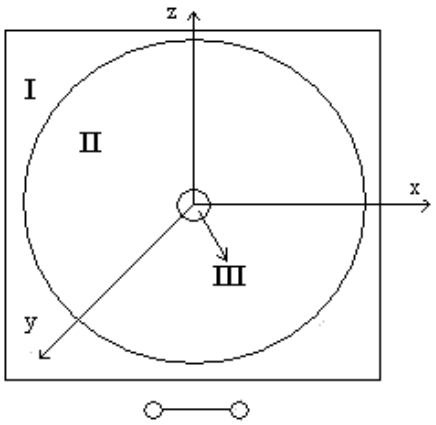

Figure 1: Simulation setup.

$$\begin{aligned} E(r) &= \frac{[I]L\cos\theta}{2\pi\epsilon_0}\left(\frac{1}{cr^2}+\frac{1}{j\omega r^3}\right) \\ E(\theta) &= \frac{[I]L\sin\theta}{4\pi\epsilon_0}\left(\frac{j\omega}{c^2 r}+\frac{1}{cr^2}+\frac{1}{j\omega r^3}\right) \\ E(\phi) &= 0 \end{aligned} \tag{1}$$

In Eq. 1, L is the length of the dipole, r is the distance of any point in the scattering domain from the dipole centre and f is the frequency of operation. The angular frequency is given by $\omega = 2\pi f$. $[I]$ is the retarded current and c is the velocity of light. Throughout our simulations $f = 6\,\mathrm{GHz}$, $L = 0.01\,\mathrm{m}$ and $[I] = 10\,\mathrm{A}$. The total field $\mathbf{E}$ will be measured on the surface of scattering domain at $z = 0.07\,\mathrm{m}$. The scattered field $\mathbf{E}^s$ is given by $\mathbf{E}^s = \mathbf{E} - \mathbf{E}^i$ where $\mathbf{E}^i$ is the incident field.

At high frequencies, to overcome the relaxation effect of complex permittivity, the single-pole Debye dispersion expression [9] is used for representing complex permittivity:

$$\tilde{\epsilon}_r(\omega) = \epsilon_r^{'}(\omega) - j\epsilon_r^{''}(\omega) = \epsilon_\infty + \frac{\epsilon_s - \epsilon_\infty}{1 + j\omega\tau} - j\frac{\sigma_s}{\omega\epsilon_0} \tag{2}$$

Here, ϵ_∞ is the relative permittivity at infinite frequency, ϵ_s is the static relative permittivity, σ_s is the static conductivity and τ is the relaxation time constant. The scattering domain in Fig. 1 has three regions with different dielectric properties as given in Table 1 [9]. Region I is outside the sphere and acts as a coupling liquid between the breast phantom and radiation source. Region II acts as the normal breast phantom and region III acts as the malignant region. Throughout the scattering domain, the permeability $\mu = \mu_0$ is constant.

Table 1: Debye parameters (in SI units) for the breast phantom in Fig. 1 at 6 GHz.

	Dielectric properties of the breast phantom					
	ϵ_∞	ϵ_s	σ_s	τ	ϵ_r	σ
Region I	4.0	10.0	0.1	7.0e-12	10	0.1
Region II	6.57	16.29	0.23	7.0e-12	15.66	1.03
Region III	3.99	54.00	0.70	7.0e-12	50.74	4.82

3. VOLUME ELECTRIC FIELD INTEGRAL EQUATION (VEFIE)

The electric field inside the scattering domain can be represented by a Fredholm integral equation of the second kind [6], given by:

$$\mathbf{E}(\mathbf{r}) = \mathbf{E}^i(\mathbf{r}) + (k_b^2 + \nabla\nabla.) \int_V G(|\mathbf{r} - \mathbf{r}'|)\chi(\mathbf{r}')\mathbf{E}(\mathbf{r}')d\mathbf{r}' \tag{3}$$

Here, $\mathbf{E}^i$ is the incident electric field and $\mathbf{E}$ is the total electric field in the scattering domain V. k_b is the wavenumber in the coupling medium given by $k_b = \omega\sqrt{\mu_b\tilde{\epsilon}_b}$, χ is the contrast function given by $\chi = \frac{k^2}{k_b^2} - 1$. $G(|\mathbf{r} - \mathbf{r}'|)$ is the scalar Green's function. Note that the harmonic time dependence $e^{-j\omega t}$ is omitted in Eq. (3) and in all equations henceforth.

4. DISCRETIZATION OF VEFIE USING CYCLIC BOUNDARY CONDITIONS

The magnetic vector potential is defined [6] as:

$$\mathbf{A} = -j\omega\mu_b\tilde{\epsilon}_b \int_V G(|\mathbf{r} - \mathbf{r}'|)\chi(\mathbf{r}')\mathbf{E}(\mathbf{r}')d\mathbf{r}' \tag{4}$$

Then the integral Eq. (3) can be written as:

$$\mathbf{E}(\mathbf{r}) - j\omega\mathbf{A} - \mathbf{E}^{irr} = \mathbf{E}^i(\mathbf{r}) \tag{5}$$

In Eq. (5), $\mathbf{E}^{irr}$ is the irrotational part of scattered electric field and is denoted as in Eq. (6).

$$\mathbf{E}^{irr} = \frac{j\omega}{k_b^2}\nabla\nabla \cdot \mathbf{A} \tag{6}$$

The scattering domain V is discretized into $N \times N \times N$ cubic cells of volume $dv = dx \times dy \times dz$. In our simulations, N is set to be equal to 21. The cell centres are located at:

$$\mathbf{r}_{j,k,l} = [j \times dx, k \times dy, l \times dz] \tag{7}$$

To mimic a continuous scattering domain, we include the cyclic boundary condition [7] in the discretization procedure. According to this condition, if the scattering domain has N cells in each direction, the Nth cell in the x-direction will be considered as the left neighbour of first cell in that direction and the first cell will be considered as the right neighbour of the Nth cell. It is likewise in the y and z directions. Testing Eq. (5) with the delta function $\delta(\mathbf{r} - \mathbf{r}_{j,k,l})$ gives the field values at $\mathbf{r}_{j,k,l}$ given by Eq. (8), where $j \in [1, J]$, $k \in [1, K]$, $l \in [1, L]$.

$$\mathbf{E}^i_{j,k,l} = \mathbf{E}_{j,k,l} - j\omega\mathbf{A}_{j,k,l} - \mathbf{E}^{irr}_{j,k,l} \tag{8}$$

The magnetic vector potential in (4) can be expressed as:

$$\mathbf{A}_{j,k,l} = -j\omega\mu_b\tilde{\epsilon}_b dv \sum_{j'=1}^{J}\sum_{k'=1}^{K}\sum_{l'=1}^{L} G_{j-j',k-k',l-l'}\chi_{j',k',l'}\mathbf{E}_{j',k',l'} \tag{9}$$

where, $j \in [1, J]$, $k \in [1, K]$, $l \in [1, L]$. The Green's function [10] is given by:

$$G_{j,k,l} = \begin{cases} \frac{(1-\frac{1}{2}jk_0dr)\exp(\frac{1}{2}jk_0dr)-1}{\frac{1}{6}\pi k_0^2 dx^3} & \text{if } |r| = 0 \\ \frac{\exp(jk_0|r|)\left[\frac{\sinh(\frac{1}{2}jk_0dr)}{\frac{1}{2}jk_0dr)} - \cosh(\frac{1}{2}jk_0dr)\right]}{\frac{1}{3}\pi(k_0dr)^2|r|} & \text{if } |r| > 0 \end{cases} \tag{10}$$

The convolution in Eq. (9) may be efficiently evaluated by applying the Fast Fourier Transform, i.e.,

$$\mathbf{A}_{j,k,l} = C\left[FFT^{-1}[FFT[G_{j',k',l'}] \cdot FFT[\chi_{j,k,l}\mathbf{E}_{j,k,l}]\right] \tag{11}$$

where $C = -j\omega\mu_b\tilde{\epsilon}_b dv$. In our simulation, the inclusion of the cyclic boundary condition reduces the number of FFTs involved by a factor $3(N+2)^3 - 3N^3$. The components of $\mathbf{E}^{irr}_{j,k,l}$ in Eq. (8) can be computed as in [6]. Eq. (8) may now be written as a matrix equation of the form

$$\mathbf{E}^i = \mathfrak{L}[\mathbf{E}] \tag{12}$$

In Eq. (12), $\mathfrak{L}$ represents the linear operations in Eq. (8) and 11 and in [6] acting on the total field $\mathbf{E}_{j,k,l}$.

5. NUMERICAL RESULTS

In order to find the unknown electric field, Eq. (12) needs to be solved numerically. Direct solution involves the inversion of a large matrix and this is prohibitive from a computational viewpoint. Consequently, iterative methods are employed for the solution of Eq. (12). We intend to use a Krylov subspace method for iteratively solving this equation. In addition, it should be noted that because of the probable non-symmetric location of tumour tissues in the breast phantom, Eq. (12) will not be symmetric. To tackle this asymmetry, we use the BI-CGSTAB-FFT method [8] to solve the matrix equation in (12). The residual error in satisfying Eq. (12) at the nth iteration step is given by $\mathbf{e}_n = \mathbf{E}^i - \mathfrak{L}[\mathbf{E}_n]$. The rate of convergence of the BI-CGSTAB-FFT method is measured as:

$$\delta_n = log\left(\frac{||\mathbf{e}_n||_2}{||\mathbf{e}_1||_2}\right) \tag{13}$$

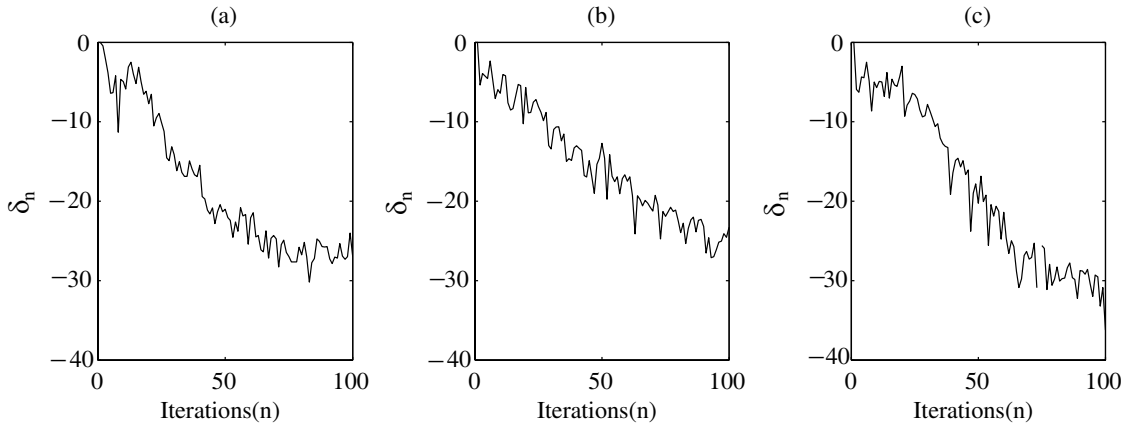

Figure 2: Rate of convergence of the BI-CGSTAB-FFT method measured as in Eq. (13), (a) with a random initial value for $\mathbf{E}$, (b) with the incident field $\mathbf{E}^i$ as the initial value for $\mathbf{E}$, (c) with the incident field $\mathbf{E}^i$ as initial value for $\mathbf{E}$ and the cyclic boundary condition.

Figure 2(a) shows the convergence rate δ_n of the BI-CGSTAB-FFT implementation when a random initial value is selected for $\mathbf{E}$. When the incident field $\mathbf{E}^i$ is used as the initial value for $\mathbf{E}$, better convergence is achieved as evident from Fig. 2(b). Fig. 2(c) shows the convergence rate when the cyclic boundary condition is employed. Note also that for Fig. 2(c), $\mathbf{E}^i$ is chosen as the initial value for $\mathbf{E}$. Comparing the figures, it is obvious that the cyclic boundary condition does not affect the convergence rate. However, in our case, it reduces the number of FFTs involved in the simulation by 23% and saves a considerable amount of memory.

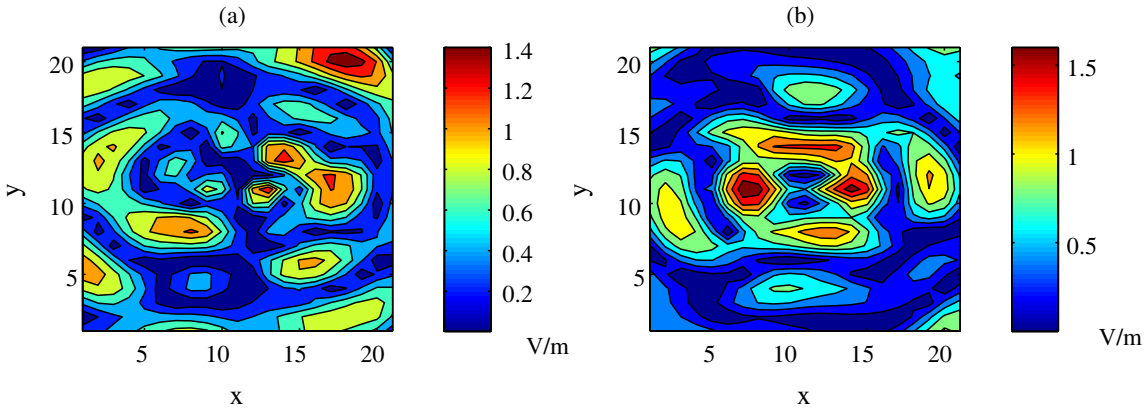

Figure 3: Scattered field $\mathbf{E}^s$ measured on the surface ($z = 0.07$ m) of the scattering domain, (a) without the tumour and (b) with the tumour.

Figure 3 shows the scattered field measured on the surface ($z = 0.07$ m) of the scattering domain, (a) without the tumour and (b) with the tumour. From Fig. 3, it is clear that the measured scattered

field on the surface of the scattering domain is different when an inhomogeneity is present inside the scatterer. The scattered field can then be used with an inversion algorithm to identify the location of the tumour.

6. CONCLUSION

Simulation of electromagnetic scattering problems at microwave frequencies is computationally challenging because of the large size of governing matrix equations. Any improvement in the formulation and algorithm that reduces the memory requirements and computation times is of immense importance. Microwave imaging is a promising alternative for mammography and other kinds of medical imaging. Simulation of these systems is computationally expensive. We have examined the inclusion of a cyclic boundary condition in the discretization procedure which indeed mimics a continuous scattering domain and reduces the overall computation by a considerable amount compared to previous works. Furthermore, in the BI-CGSTAB iteration method, we proposed the selection of the incident electric field itself as the initial condition for solving for the total field. Results confirm that it gives better convergence when compared to the standard choice of initial condition.

ACKNOWLEDGMENT

This work was funded by Science Foundation Ireland

REFERENCES

1. MARIBS study group, "Screening with magnetic resonance imaging and mammography of a UK population at high familial risk of breast cancer: A prospective multicentre cohort study (MARIBS)," *The Lancet*, Vol. 365, 1769–1778, May 16, 2005.
2. Khor, W. C., et al., "An ultra wideband microwave imaging system for breast cancer detection," *IEICE Transactions on Communication*, Vol. E90-B, No. 9, 2376–2380, 2007.
3. Chaudhary, S. S., et al., "Dielectric properties of normal and malignant human breast tissues at radiowave and microwave frequencies," *Indian J. Biophys*, Vol. 21, No. 10, 76–79, 1984.
4. Lazebnik, M., et al., "A large-scale study of the ultrawideband microwave dielectric properties of normal, benign, and malignant breast tissues obtained from cancer surgeries," *Physics in Medicine and Biology*, Vol. 52, 6093–6115, 2007.
5. Krauss, J. D., *Antennas 2ed.*, Mc Graw-Hill, New York, 1998.
6. Zhang, Z. Q., et al., "Microwave breast imaging: 3-D forward scattering simulation," *IEEE Transactions on Biomedical Engineering*, Vol. 50, No. 10, 1180–1188, 2003.
7. Johnson, H. J. and G. E. Christensen, "Consistent landmark and intensity-based image registration," *IEEE Transactions on Medical Imaging*, Vol. 21, No. 5, 450–461, 2002.
8. Van der Vorst, H. A., "BI-CGSTAB: A fast and smoothly converging variant of BI-CG for the solution of nonsymmetric linear systems," *SIAM J. Sci. Statist. Comput.*, Vol. 13, 631–644, March 1992.
9. Converse, M., et al., "A computational study of ultrawideband versus narrowband microwave hyperthermia for breast cancer treatment," *IEEE Transactions on Microwave Theory and Techniques*, Vol. 54, 2169–2180, 2006.
10. Zwarmborn, P. and P. van den Berg, "The three dimensional weak form of the conjugate gradient FFT method for solving scattering problems," *IEEE Transactions on Microwave Theory and Techniques*, Vol. 40, 1757–1766, 1992.